Video Article

Setting-up an *In Vitro* Model of Rat Blood-brain Barrier (BBB): A Focus on BBB Impermeability and Receptor-mediated Transport

Yves Molino[1], Françoise Jabès[1], Emmanuelle Lacassagne[2], Nicolas Gaudin[2], Michel Khrestchatisky[2]

[1]VECT-HORUS SAS

[2]Aix-Marseille Université, CNRS, NICN UMR 7259

Correspondence to: Michel Khrestchatisky at michel.khrestchatisky@univ-amu.fr

URL: https://www.jove.com/video/51278
DOI: doi:10.3791/51278

Keywords: Medicine, Issue 88, rat brain endothelial cells (RBEC), mouse, spinal cord, tight junction (TJ), receptor-mediated transport (RMT), low density lipoprotein (LDL), LDLR, transferrin, TfR, P-glycoprotein (P-gp), transendothelial electrical resistance (TEER),

Date Published: 6/28/2014

Citation: Molino, Y., Jabès, F., Lacassagne, E., Gaudin, N., Khrestchatisky, M. Setting-up an *In Vitro* Model of Rat Blood-brain Barrier (BBB): A Focus on BBB Impermeability and Receptor-mediated Transport. *J. Vis. Exp.* (88), e51278, doi:10.3791/51278 (2014).

Abstract

The blood brain barrier (BBB) specifically regulates molecular and cellular flux between the blood and the nervous tissue. Our aim was to develop and characterize a highly reproducible rat syngeneic *in vitro* model of the BBB using co-cultures of primary rat brain endothelial cells (RBEC) and astrocytes to study receptors involved in transcytosis across the endothelial cell monolayer. Astrocytes were isolated by mechanical dissection following trypsin digestion and were frozen for later co-culture. RBEC were isolated from 5-week-old rat cortices. The brains were cleaned of meninges and white matter, and mechanically dissociated following enzymatic digestion. Thereafter, the tissue homogenate was centrifuged in bovine serum albumin to separate vessel fragments from nervous tissue. The vessel fragments underwent a second enzymatic digestion to free endothelial cells from their extracellular matrix. The remaining contaminating cells such as pericytes were further eliminated by plating the microvessel fragments in puromycin-containing medium. They were then passaged onto filters for co-culture with astrocytes grown on the bottom of the wells. RBEC expressed high levels of tight junction (TJ) proteins such as occludin, claudin-5 and ZO-1 with a typical localization at the cell borders. The transendothelial electrical resistance (TEER) of brain endothelial monolayers, indicating the tightness of TJs reached 300 ohm·cm^2 on average. The endothelial permeability coefficients (Pe) for lucifer yellow (LY) was highly reproducible with an average of 0.26 ± 0.11 x 10^{-3} cm/min. Brain endothelial cells organized in monolayers expressed the efflux transporter P-glycoprotein (P-gp), showed a polarized transport of rhodamine 123, a ligand for P-gp, and showed specific transport of transferrin-Cy3 and DiILDL across the endothelial cell monolayer. In conclusion, we provide a protocol for setting up an *in vitro* BBB model that is highly reproducible due to the quality assurance methods, and that is suitable for research on BBB transporters and receptors.

Video Link

The video component of this article can be found at https://www.jove.com/video/51278/

Introduction

Many drugs developed to treat Central Nervous System (CNS) disorders are unable to reach the brain parenchyma in therapeutically relevant concentrations. The BBB protects brain nervous tissue from the fluctuation of plasma composition, from pathogenic agents, and maintains homeostasis of the brain parenchyma by restricting non-specific flux of ions, peptides, proteins and even cells into and out the brain[1].

BBB characteristics are induced and maintained by intimate proximity and cross-talk between the specialized class brain microvessel endothelial cells and neighboring elements of the neuro-glia-vascular unit (NGVU) such as neurons, glial cells (more precisely astrocyte end-feet), and pericytes ensheathed in the basal membrane which consists mainly of collagen type IV, fibronectin, laminin and proteoglycans[2,3]. Pericytes cover approximately 22 - 32% of the endothelium at the capillary level and play an important role in the regulation of endothelium proliferation, angiogenesis and inflammatory processes. Endothelial cells form a continuous sheet covering the inner surface of the capillaries. They are interconnected by TJs, which form a belt-like structure at the apical region and that contribute to cell polarization. Astrocytes regulate BBB properties and are sources of important regulatory factors such as TGF-β, GDNF, bFGF and IL-6. Astrocytes deficient in GFAP with incomplete functionality are not able to regulate BBB properties[4]. Neurons are not directly involved structurally in the formation of the BBB but also regulate important aspects of protein expression and BBB functions[5].

In order to further study the structure, physiology and pathology of the BBB, *in vitro* models of the BBB were developed as research tools. Brain endothelial cells have been extracted from various species to implement *in vitro* BBB models based on low passage primary cultures from bovine[6,7], porcine[8,9], rat[10,11,12], mouse[13] and also human[14,15]. These models are known to mimic the *in vivo* BBB, particularly when co-cultured with glial cells from rat or murine and/or pericytes[16,12], and/or neural progenitor cell-derived astrocytes[17] and/or neurons[18]. The “in lab” models are often produced from rodents because they allow *in vitro* / *in vivo* experiments and comparisons and/or the study of brain endothelial cells produced from transgenic models[19].

Newly developed *in vitro* BBB models have also been designed to help predict brain uptake of potential CNS drug candidates prior to *in vivo* testing[15,20,21,3,6,22,11,23]. *In vitro* BBB models are usually used to compare the transport of drugs with: i) known penetration into the CNS or with low permeability across the BBB and no central effects, and ii) the apparent Pe of the same drugs measured in animal models of the same species. The drugs that readily pass the BBB are mostly lipophilic and cross the brain endothelial cell membranes by lipid-mediated free diffusion (caffeine, carbamazepine, etc.). The negatively transported drugs such as digoxin, verapamil or cyclosporine A are actively extruded by brain endothelial efflux transporters such as P-gp. However, many of the newly developed therapeutic molecules are biopharmaceuticals, such as recombinant proteins, siRNAs or monoclonal antibodies. Most of them do not cross the BBB due to: i) the absence of specific transporters, and ii) the tightly packed layer of endothelial cells, which prevent high molecular weight molecules from undergoing paracellular passage. With these limits, “Trojan horse” strategies have been implemented using vectors (antibodies, peptides) against known receptors at the BBB, involved in receptor mediated transport or transcytosis (RMT), such as the transferrin (Tf) receptor (TfR), the Insulin receptor (IR), or members of the LDL receptor (LDLR)-related receptor family (LDLR, LRP1). Such receptors have been found on isolated brain capillaries and in the BBB *in vivo*[24,25]. Transcriptional profiles for these receptors, in particular those of the LDLR family, were analyzed and compared between brain endothelial cells and brain endothelial cells co-cultured with astrocytes or in brain capillaries directly after their extraction from brain[26]. Pardridge[24] opened the field with the OX-26 antibody against the transferrin receptor (TfR), followed by antibodies against the insulin receptor and the insulin growth factor receptor[27,28]. With these antibody based vectors, ArmaGen Technologies has developed a BBB molecular Trojan horse platform technology to deliver drugs, including proteins, across the BBB[29]. The literature is rich in data showing LRP1 expression in brain endothelial cells and its role as a powerful endocytic/scavenger receptor. Western blot analysis suggested that LRP1 is expressed in fractions enriched in brain capillaries and in rat brain capillary endothelial cells[30]. Companies such as Angiochem target LRP1 with peptide vectors derived from aprotinin that promote efficient drug influx across the BBB[31]. However, LRP1 is also involved in active transport of Aβ and its efflux/clearance from brain parenchyma to blood[32]. Such data involve LRP1 in a bi-directional transport across the BBB depending on its ligands. biOasis develops the Transcend technology using a protein melanotransferrin for the transport of biologics such as lysosomal enzymes and antibodies across the BBB[33] while VECT-HORUS develops peptide vectors that target the LDLR[34]. There is data suggesting that the LRP and LDLR can be used to transport different molecules such as lysosomal enzymes[35,36] or nanoparticle complexes across the BBB[37].

Our field of interest is drug delivery to the CNS using vector molecules and vectorized drug-candidates for the treatment of CNS diseases. In particular, drug delivery across the BBB has to be considered within the context of neuroinflammation, a process that may vary in its extent, but that is probably common to all CNS lesions and diseases, including encephalitis, multiple sclerosis, Alzheimer’s disease etc. Neuroinflammation is associated with BBB inflammation and potentially with changes in BBB physiology and permeability considering that paracellular and transcellular transport can be amplified in pathological conditions[38,39,40,41,42,43]. For instance, TNF-α, TWEAK, and other cytokines modulate inflammation, and experiments with *in vitro* BBB models have shown that they can alter the paracellular properties of the endothelial cell monolayer[38,39,40] and that TNF-α also leads to an increase in transcellular transport of LDL[41], holotransferrin[42] and lactoferrin[43].

Our objective was to develop and characterize an optimized and highly reproducible rat syngeneic BBB model using co-cultures of primary brain endothelial cells and astrocytes. We used 5 week old and neonatal Wistar rats for brain endothelial cell production and astrocyte production respectively. One challenge was to establish a protocol allowing the production of “weekly reproducible” BBB models. To reach this objective, every step of the production protocol was performed on fixed days of the week, starting from brain microvessel production on Wednesday of the first week. Dissections were performed nearly every week during the last 3 years. To further improve the reproducibility of the cultures, a quality assurance system was established. All reagents and chemicals were referenced in a database (date of entry, stock, expiration term, etc.).

The model was characterized following a number of criteria, such as endothelial cell organization and purity, TEER, LY permeability, response to pro-inflammatory agents, qualitative and quantitative expression of TJ proteins, functionality of efflux transporters such as P-gp, and receptors involved in transcytosis across the endothelial cell monolayer such as the TfR or the LDLR.

Protocol

1. Production of Rat Astrocytes

For each preparation use 10 neonatal Wistar rats of either sex.

1. Sacrifice the rats by cutting heads with a pair of scissors and transfer them immediately in a dry Petri dish under a laminar flow hood. Remove the brains from the skull without the cerebellum and transfer them immediately into a Petri dish containing cold dissection buffer: HBSS supplemented with 1% Bovine Serum Albumin (low level of endotoxin BSA), penicillin 100 units/ml and streptomycin 100 µg/ml.
2. Cut the brains in half, to separate the 2 cerebral hemispheres and transfer them into a clean Petri Dish with dissection buffer on ice. Cut the optic nerve and remove the meninges under a stereomicroscope.
3. Wash the cortical pieces extensively in 50 ml of cold dissection buffer.
4. Place the cortical pieces from 3 brains into a 15 ml Falcon tube and dissociate by pipetting up and down a couple of times with a 10 ml disposable pipette equipped with a blue tip into 6 ml of trypsin 0.05% - EDTA 0.02% for 5 min at 37 °C.
5. Add 24 ml of DMEM supplemented with 10% FBS and the following antibiotics, penicillin 100 units/ml and streptomycin 100 µg/ml, a media named glial cell media (GCM), and centrifuge at 300 x g for 5 min at RT. FBS batches were selected and validated for the growth and survival of astrocyte cutures.
6. Resuspend the pellet containing the dissociated cells in 10 ml GCM and plate into a 75 cm^2 T-flask (T75). Change the medium the following day to remove the cell debris and DNA. Replace the culture media twice a week.
7. After 1 week of proliferation, gently shake the glial cells with an orbital shaker at 60 rpm during 24 hr at 37 °C in GCM. If the T75 cannot be placed in an incubator with 5% CO_2 / 95% air at 37 °C humidified atmosphere, supplement the media with 5 mM HEPES. Wash the cells twice to remove the non-adherent microglial cells.
8. Three weeks after seeding, wash the cells twice with DPBS without calcium and magnesium. Add 3 ml of warm trypsin 0.05%-EDTA 0.02%, incubate at 37 °C and wait until the cell layer is dispersed (usually 5 min). Inhibit trypsin activity by adding 10 ml of GCM, transfer the cell suspension into a 15 ml Falcon tube and centrifuge at 120 x g for 8 min.

9. Resuspend the astrocyte pellet in 90% FBS – 10% DMSO, transfer them into cryovials (2 x 10^6 cells per cryovial) and store in liquid nitrogen.

2. Isolation of Rat Brain Microvessels

Our experimental procedures are approved by the Ethics Committee of the Medical Faculty of Marseille and conform to National and European regulations (EU directive No. 86/609). All efforts were made to minimize animal suffering and reduce the number of animals used.

1. For each preparation and for one experimenter, use 3 five week old Wistar rats.
2. Monday of the first week, prepare 2 T75 flasks by coating with collagen type IV and fibronectin, both at 1 µg/cm^2 in sterile culture water (10 ml per T75). Allow to adhere at 37 °C until microvessel seeding.
3. Wednesday morning of the first week, euthanize the rats under an increasing flux of CO_2 to induce drowsiness, loss of posture and breathing interruption, then followed by a cervical dislocation. Spray the heads with 70% ethanol. Cut the heads with a pair of scissors and transfer them into a dry Petri dish under a laminar flow hood.
4. Remove the brains from the skull without the cerebellum and the optic nerves, then transfer them into a Petri dish cooled on ice and filled with cold dissection buffer (HBSS supplemented with 1% BSA, penicillin 100 units/ml and streptomycin 100 µg/ml).
5. Cut the brains in half to separate the 2 cerebral hemispheres and separate midbrain from forebrain. Transfer the forebrains into a clean Petri dish on ice with dissection buffer.
6. Take a couple of hemispheres in a new Petri dish with cold dissection buffer to carefully remove the meninges from the forebrains under a stereomicroscope with N° 5 curved forceps. Then, clean the interior of the brain to remove the duvet of myelin and obtain a shell of cortex. These steps should not take more than 2 hr for tissue preservation and cell survival.
7. Dissociate the cortex from 3 brains into 6 ml of cold dissection buffer in a 7 ml dounce homogenizer by 10 up and down strokes with each of 2 pestles of different clearances, 71 µm followed by 20 µm.
8. Divide the suspension to obtain the equivalent of 1 cortex in 1 ml of a 50 ml Falcon tube and centrifuge at 1,000 x g for 5 min at RT. Discard the supernatant.
9. Digest the suspension from 1 cortex with 1 ml of an enzymatic solution containing a mix of collagenases / dispase (60 µg/ml – 0.3 U/ml), DNase type I (35 µg/ml – 20 K units/ml) and gentamicin (50 µg/ml) in a shaker for 30 min at 37 °C.
10. Mix the 1 ml digest from 1 cortex with 10 ml of 25 % BSA/HBSS 1X and separate by density dependent centrifugation at 3,600 x g for 15 min at RT. Carefully transfer the upper disk (myelin and brain parenchyma) and the supernatant into a clean 50 ml Falcon tube and repeat the centrifugation. Keep the resulting pellet containing the brain microvessels at 4 °C.
11. Carefully discard the upper disk and the supernatant. Resuspend both resulting pellets containing the brain microvessels with 1 ml of cold HBSS 1X and transfer into a clean 50 ml Falcon tube.
12. Wash the microvessels by addition of 20 ml of cold HBSS 1X and centrifuge at 1,000 x g for 5 min. Discard the supernatant.
13. Further digest the microvessels from 1 cortex with 1 ml of the same enzymatic solution as described in step 2.9 during 1 hr at 37 °C in a shaker.
14. Then, mix the digested microvessels from each of the 3 cortices into one tube and further separate into two 50 ml Falcon tubes to obtain microvessels extracted from the equivalent of one and a half (1.5) cortex per tube. Add 30 ml of cold dissection buffer and centrifuge at 1,000 x g for 5 min at RT.
15. Resuspend the microvessel pellet in 10 ml of DMEM/F12 supplemented with 20% bovine platelet poor plasma derived serum, basic fibroblast growth factor (bFGF, 2 ng/ml), heparin (100 µg/ml), gentamicin (50 µg/ml) and HEPES (2.5 mM), named endothelial cell media (ECM) supplemented with puromycin at 4 µg/ml.
16. Take the 2 coated T75 flasks from the incubator, aspirate the excess of coating and plate the microvessels from each tube in one T75 flask (microvessels extracted from 1.5 cortex per T75 flask).

3. Purification and Proliferation of RBEC Primocultures

1. Purification: Wednesday to Friday, add puromycin at 4 µg/ml to the culture media. Change the medium on Thursday. On Friday, wash the cells and add puromycin at 2 µg/ml until Monday.
2. Proliferation: on Monday of the second week, wash the cells and add insulin, transferrin and sodium selenite supplement to the culture media until the cultures reach 90% confluence on Wednesday of the second week.

4. Differentiation: Setting up the *In Vitro* BBB Model

1. Monday of the second week, prepare filters (polyethylene, 12 wells, pore size 1.0 µm) by coating with a mix of collagen type IV and fibronectin both at 0.5µg/cm^2 in sterile culture water (500 µl of mix in the upper compartment and 1.5 ml of sterile culture water in the lower compartment). Allow to adhere at 37 °C until RBEC seeding.
2. Monday of the second week, five days before the establishment of the co-culture, thaw the astrocytes from cryovials at 37 °C and transfer in a 15 ml Falcon with 10 ml GCM. Centrifuge the suspension at 120 x g for 8 min at RT.
3. Resuspend the astrocyte pellet in GCM and plate at a density of 30 x 10^3 cells per cm^2 in 12-well plates.
4. Wednesday of the second week, just before dissociation of RBEC with trypsin, wash twice the pre-coated filter with DMEM/F12 medium. Pre-fill the chambers with ECM: 1.5 ml in the lower compartment and 0.5 ml in the upper compartment.
5. Wednesday of the second week, wash twice the RBEC with DPBS without calcium and magnesium. Add 4 ml of warm trypsin 0.05% - EDTA 0,02% solution at 37 °C per T75 flask during 30 sec exactly. Then remove 3.5 ml of trypsin solution and observe under the microscope. When the cell layer starts to detach from the matrix, help them by gently tapping the edge of the T75 flask until all the cells are floating.
6. Add 9 ml of ECM per T75 flask and transfer into a 15 ml Falcon tube. Very gently dissociate the cell suspension by pipetting up and down 4 times with a 10 ml pipette equipped with a yellow tip (avoid the production of bubbles in the solution). Count the cells in the suspension (approximately 3 x 10^6 cells/T75) and immediately plate on pre-coated and pre-filled filters at a high density (160 x 10^3 cells/filter hence approximately 18 filters/T75) (**Figure 8**). The following day (Thursday), change twice the medium of the upper compartment to remove cell debris.

7. Thursday of the second week, the day before the establishment of the co-culture, replace the astrocyte culture media by 1.5 ml of differentiation media (ECM with hydrocortisone at 500 nM) that can be supplemented with 1/3 conditioned medium from the basal compartment of a previous co-culture (3 days of contact between endothelial cells and astrocytes).
8. Friday of the second week is defined as the day 0 of differentiation; replace the culture media from the filters containing the RBEC with differentiation media. Transfer the RBEC filters into the wells containing the astrocytes. Under these conditions, *in vitro* models differentiate and express junction-related proteins within 3 days.
9. The models keep their optimal differentiation during 3 more days, between Monday and Wednesday of the third week.

Representative Results

Production Protocol
The protocol can be divided into 3 phases corresponding to major changes in culture media composition: (a) purification of endothelial cells from the microvessels, (b) proliferation, and (c) differentiation on filters (12-well polyethylene plates with a porosity of 1 µm) in co-culture with astrocytes. The different steps of the production protocol were assigned to specific days of the week in order to increase the reproducibility of the primary cell cultures (**Figure 1**). On Wednesday of the first week, hence 9 days before the establishment of the co-culture system, the microvessels were isolated (**Figure 2A**). To purify endothelial cells, the cultures were kept in the presence of decreasing concentrations of puromycin for 5 days. Most contaminating cells (mainly pericytes) were eliminated and the growth of endothelial cells was slower without modification of their phenotype. Spindle-shaped cells grow out of the capillary fragments isolated from rat brain grey matter (**Figure 2B**).
On Monday of the second week, rat astrocytes were plated on the bottom of 12-well plates. Wednesday, RBEC were added to the luminal compartment of the filters. High density seeding at 160 x 10^3 cells/cm^2 (**Figure 2C**) helps to avoid gaps at the periphery of the filter (**Figure 2D**) and generates a homogeneous differentiation of the endothelial cell monolayer. The cells show the typical elongated spindle-shaped morphology, align longitudinally, and form a uniform monolayer. Thursday, astrocyte culture medium was changed for the differentiation medium conditioned with the previous co-culture media (**Figure 2E**). Friday, RBEC on filters were grown in culture medium containing 500 nM hydrocortisone and the filters were transferred to 12-well plates containing the astrocytes. On the third week, experiments were performed between Monday and Wednesday.

RBEC Characterization and Determining Elements of Monolayer Permeability
The RBEC were characterized by immunostaining of endothelial and BBB markers as well as by measurements of TEER, permeability of LY and functionality of efflux transporters such as P-gp.

RBEC obtained by the puromycin purification method (**Figure 1** and **2**) grew in non-overlapping continuous monolayers that exhibited growth inhibition at confluence and displayed tightly apposed, fusiform and spindle shaped morphology. RBEC cultures expressed typical markers of endothelial cells: they showed positive immunostaining for platelet endothelial cell adhesion molecule (**Figure 3A**; CD31/PECAM) and expression of von Willebrand factor (**Figure 3B**). Without puromycin treatment, RBECs are quickly invaded by pericytes detected by desmin immunostaining (**Figure 3C**). Glial fibrillary acidic protein (GFAP) expressed by astrocytes (**Figure 3D**) is an important differentiation marker of astrocytes. With high passage number, astrocytes lose their ability to induce differentiation of the endothelial cells. For this reason, astrocyte cultures were standardized for their time of culture and only underwent one passage.

Culturing RBEC with media supplemented with hydrocortisone, followed by co-culture with astrocytes and with conditioned medium from the lower compartment of previous co-cultures led to strong induction of interendothelial TJs in comparison to RBEC cultured alone. The cells expressed claudin-5, ZO-1 and occludin proteins, which were localized at the cell-cell junctions, as shown by immunofluorescence (**Figure 4B-D**) and revealed by western blot analysis for ZO-1 and occludin proteins (**Figure 4E**). The morphological distribution at cell-to-cell contacts in a zipper-like configuration reflects (a) the tightness of the monolayer, (b) the cerebral origin of the capillary endothelial cells, and (c) is characteristic of highly differentiated cerebral endothelial cells. Paracellular permeability of the endothelial layer was monitored by measuring the TEER and the rate of influx of LY (457 Da) from the upper to the lower compartment of the filters. TEER was measured using an ENDOHM-12 for 12 mm culture cups connected to an EVOM voltohmmeter. The TEER of brain endothelial monolayers, indicating the tightness of TJs reached 300 ohm · cm^2 on average (filters of 12 well plates, data not shown). The Pe for LY ($Pe_{(LY)}$, used as an integrity control of the barrier and co-incubated with tested compounds) reached an average of 0.26 ± 0.11 x 10^{-3} cm/min (**Figure 4F**) over a 1 year period.

In order to induce inflammation of RBEC we used the pro-inflammatory cytokine TNF-α at 5 ng/ml for 24 hr, and followed the inflammatory response by measuring CCL2 (MCP-1) secretion by RBEC in the upper compartment of the culture system which doubled from 120 ng/ml (non-treated control) to 250 ng/ml (**Figure 5A**). TNF-α treatment at 5 ng/ml or 50 ng/ml for 24 hr also opened the BBB as revealed by $Pe_{(LY)}$ measurement (**Figure 5B**) .

P-gp was visualized in differentiated RBEC by immunocytochemistry (**Figure 6A**). P-gp localization is known to be highly polarized and expressed essentially in the apical membrane of endothelial cells[44] while the Glutamate transporter-1 (GLT-1) is mainly found in the basolateral fraction[45]. To assess the extent of polarization of our cultured RBEC, apical and basolateral proteins were separated from plasma membrane preparations using sucrose density gradients[46]. Western blot analysis was performed to assess expression levels of P-gp and GLT-1 in plasma, apical and basal membrane preparations. Microvessels freshly extracted from rat brain were used as the closest positive controls to the *in vivo* distribution of these proteins (**Figure 6B**). In both microvessels and differentiated RBEC membrane preparations, P-gp was expressed as a band of 170 kDa, mainly localized in the F1 apical membrane fraction (**Figure 6B, C**). GLT-1 expression was indeed expressed in the F3 basal membrane fraction of microvessels as a band of 65-70 kDa, but was not detected in the cultured RBEC.

In parallel experiments, the functional activity of P-gp in the endothelial cell monolayer was tested using rhodamine 123 (R123) as a ligand. The abluminal to luminal (B to A) efflux of R123 was 1.7 times higher than in the opposite direction (**Figure 6D**). To prove P-gp involvement, we used specific P-gp inhibitors, verapamil (25 µM, 30 min preincubation) and cyclosporine A (1 µM, 30 min preincubation). With verapamil and cyclosporine treatment, R123 accumulation in RBEC was increased 1.6 fold and 2 fold respectively, compared to untreated control (**Figure 6E**).

Receptors Involved in Receptor Mediated Transcytosis (RMT) Mechanisms

The model was further characterized for expression of different receptors potentially involved in transcytosis mechanisms at the BBB, such as the LRP1, LDLR or TfR (**Figure 7A**).

Functional transport studies were performed with the ligands for TfR and LDLR. Live RBEC were incubated with rat transferrin labelled with CY3 (Tf-Cy3) for 180 min at 37 °C (**Figure 7B, C**). Quantification of Tf-Cy3 uptake and transport in the rat *in vitro* BBB model showed that the slope of the curves slightly decreased beyond 2,400 picomoles (**Figure 7B**), suggesting that binding/uptake was saturable. Moreover, the saturation of the binding/uptake was correlated with the accumulation of Tf in the lower compartment. To confirm this observation, Tf-Cy3 was incubated at 1,200 picomoles (ascending part of the curve) with an excess of non-fluorescent Tf at 4,800 picomoles (plateau/saturation) (**Figure 7C**). These experiments showed a decrease of Tf-Cy3 accumulation in the lower compartment and confirmed a saturable mechanism typical of ligand-receptor interaction in our *in vitro* BBB model.

Similarly, LDLR functionality was demonstrated by the uptake and transport of its ligand DiILDL across the endothelial cell monolayer (**Figure 7D, E**). Live RBEC were incubated with DiILDL for 30 min at 37 °C. The binding/uptake was not correlated with the accumulation of DiILDL in the lower compartment (**Figure 7D**). Quantification of DiILDL transport showed that the slope of the curves decreased beyond 2 µg, suggesting that transport was saturable and receptor-related in our model. Sodium azide was added at 0.05%, 15 min prior to DiILDL incubation (**Figure 7E**). The absence of toxicity of sodium azide incubation at 0.05% was assessed by $Pe_{(LY)}$ measurement (data not shown). These experiments showed decreased DiILDL accumulation in the lower compartment. Overall, our results suggest RMT for DiILDL in our *in vitro* BBB model.

Other *In Vitro* BBB Models based on Endothelial Cells from Rat spinal Cord or Mouse Brain

Enzymatic digestion with a mix of collagenases / dispase is one of the major parameters to control in terms of cell viability and production yield of cerebral microvessels. The concentration of enzyme and more important the ratio between the quantity of enzyme relative to tissue, needs to be calibrated precisely between rat brain, rat spinal cord and mice brain. Microvessel seeding density and number of endothelial cells to reach 90% confluence (9 days post microvessel seeding) were linked and are important parameters to improve cell growth, limit the number of population doubling and the quality of the models. Rat spinal cord microvessels were produced with the same protocol as the one described herein for rat brain microvessels (in terms of tissue amount, 2 spinal cords corresponding approximately to 1 brain) to obtain the same quantity of cells per T75 flask within the same time scale. Meninges from 5-week-old C57Bl6 mice brain were difficult to eliminate because they stick to the cortex. A brief treatment of the brain with dispase appears to facilitate removal of the meninges. The important parameters that contribute to the production of reproducible endothelial cell monolayers from rat brain, rat spinal cord and mouse brain are highlighted and summarized in **Figure 8**.

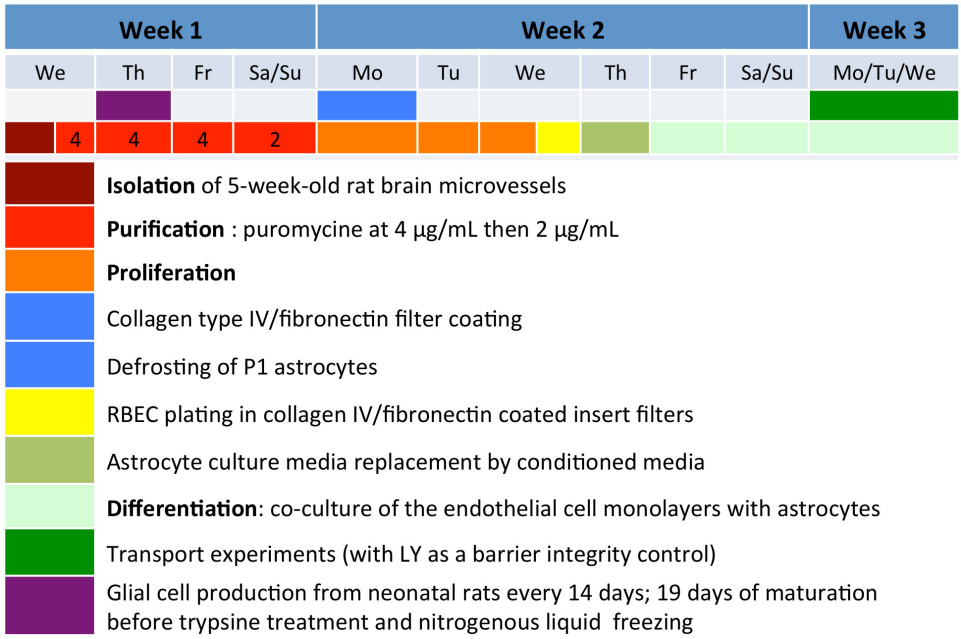

Figure 1. Flow chart summarizing the main steps of the *in vitro* BBB model preparation. The different steps of the production protocol were assigned to specific days of the week in order to increase the reproducibility of the primary endothelial cell cultures. The protocol starts on Wednesday of the first week, with microvessel production from 5-week-old Wistar rats.

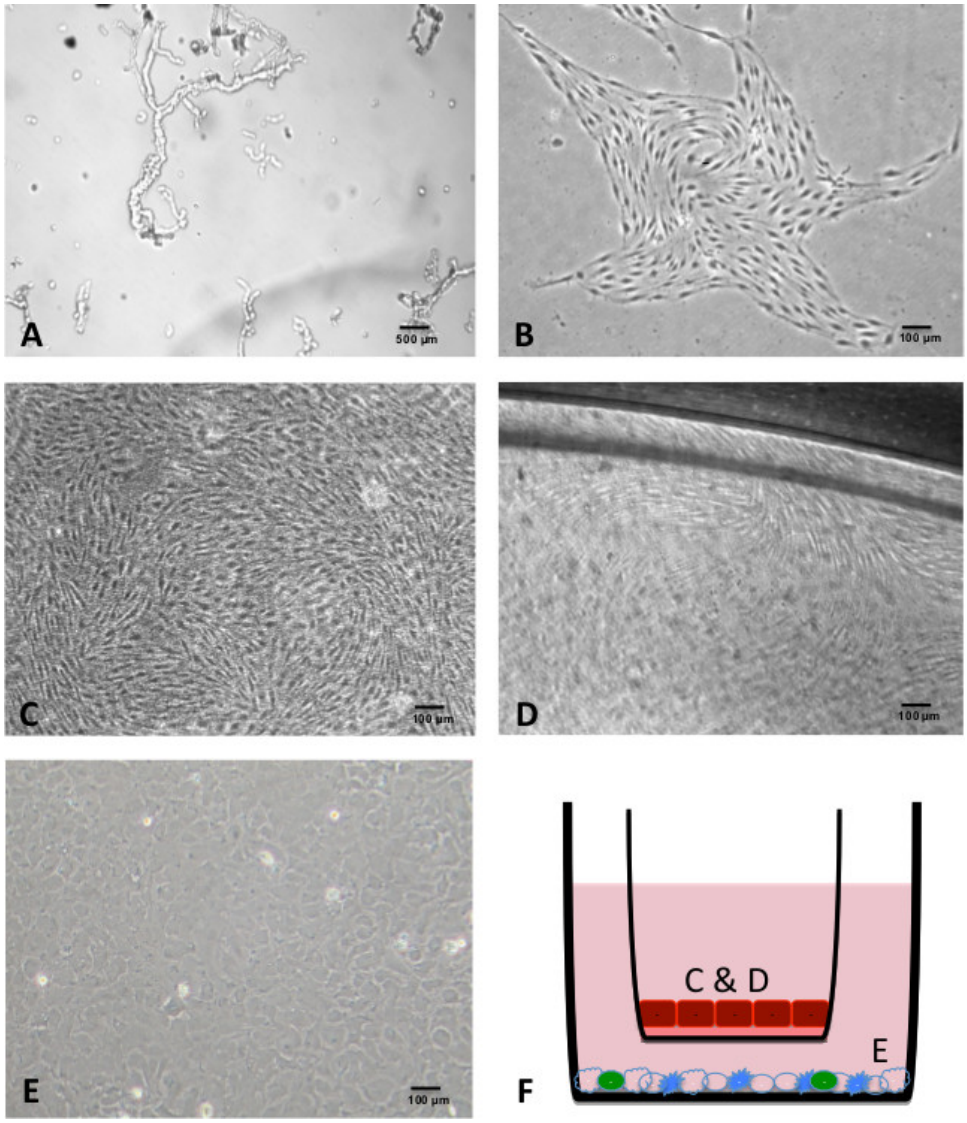

Figure 2. Phase contrast photomicrographs of RBEC, astrocytes and the co-culture system. (A) 5-week old Wistar rat microvessel fragments at the time of plating out. **(B)** Three day old RBEC cultures treated for 2 days with the P-gp substrate puromycin at 4 µg/ml. **(C)** Pure confluent endothelial monolayers at day 1 after plating on the Millipore filters of a 12 well plate coated with collagen type IV and fibronectin. **(D)** Homogeneity of the cell monolayer at the periphery of the insert filter. **(E)** Confluent astrocyte culture on the day of establishment of the co-culture showing characterized honeycomb morphology. **(F)** Scheme representing the co-culture system with localization of the photomicrographs in C, D and E.

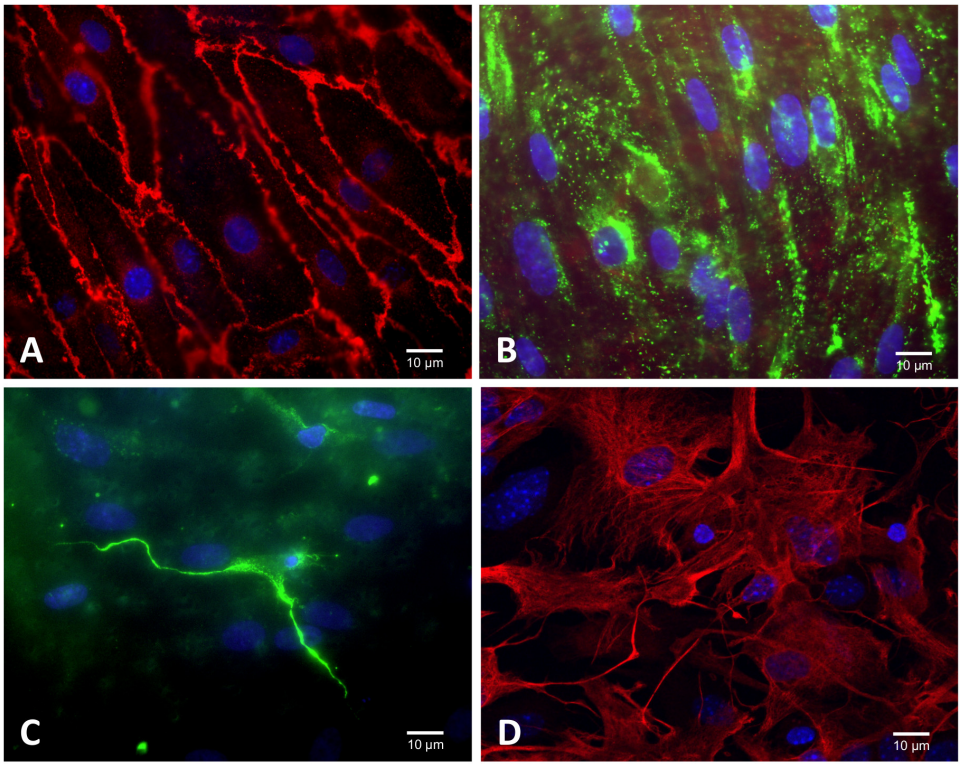

Figure 3. Characterization of RBEC cultures by immunofluorescence microscopy. (A) Brain endothelial cells express platelet endothelial cell adhesion molecule PECAM/CD31 at the cell border, **(B)** von Willebrand factor (VWF) shows a relatively punctate staining, brighter and more aggregated in some cells than others, and concentrated in the perinuclear zone. **(C)** Without puromycin treatment of RBEC cultures, pericytes are detected with a positive immunostaining for desmin (in green) and have characteristic small round nuclei. **(D)** Astrocytes express glial fibrillary acidic protein (GFAP). Please click here to view a larger version of this figure.

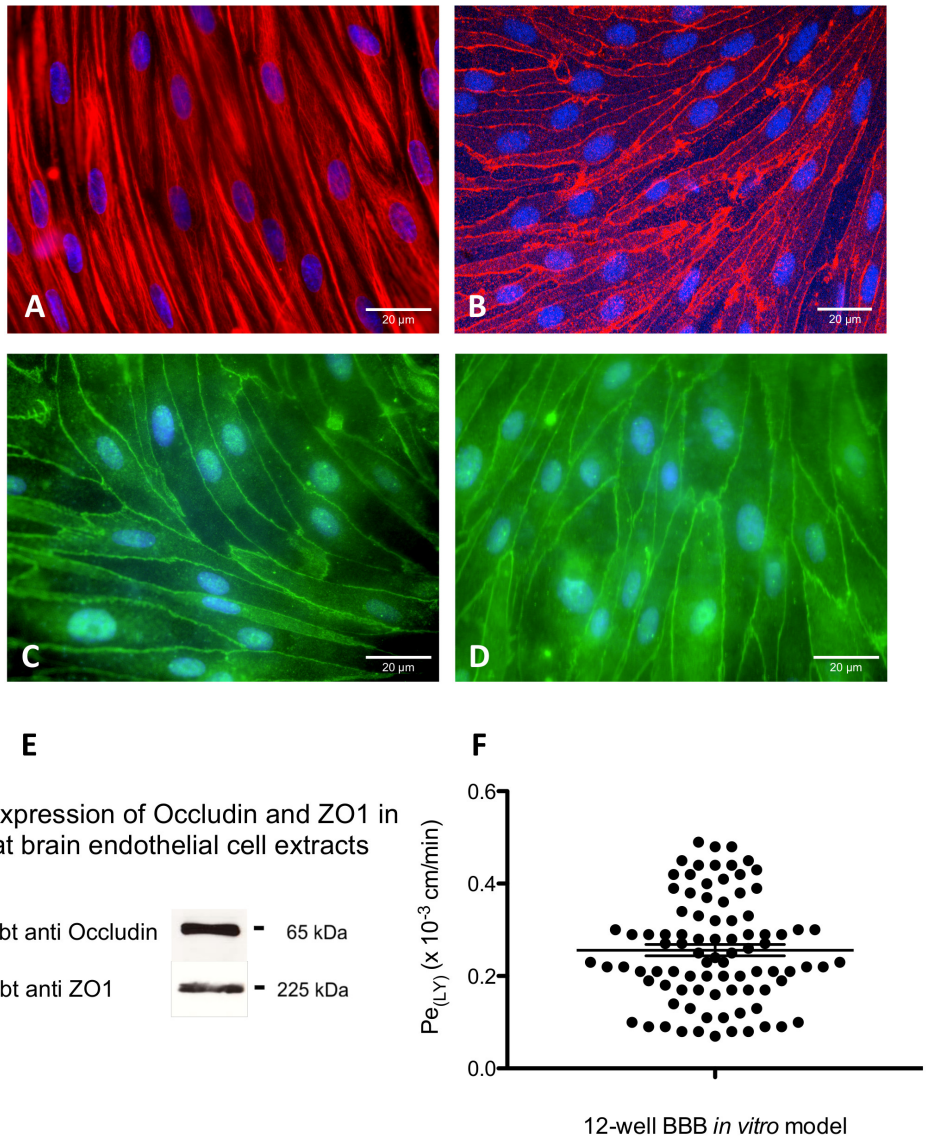

Figure 4. Immunocytochemical characterization of the rat *in vitro* BBB model and the paracellular permeability of LY across the endothelial monolayer. The cell monolayer was immunostained with **(A)** vimentin to reveal a confluent brain endothelial cell monolayer with non-overlapping morphology and typical spindle shaped cells with endothelial morphology and the expression of tight junction proteins **(B)** claudin-5, **(C)** ZO-1 and **(D)** occludin, also detected by western blot for ZO-1 and occludin proteins **(E)**. **(F)** Monolayer tightness in the 12-well BBB model was assessed by measuring the transport of lucifer yellow (LY-CH, dilithium salt), a small hydrophilic molecule (MW 457 Da) known to be retained by the BBB. Briefly, LY was incubated in the upper compartment of the culture system in contact with cerebral endothelial cells for 60 min at 37 °C. After this time, the medium of the lower compartment was collected and fluorescence was quantified by fluorimetric analysis with a spectrofluorimeter with excitation at 430 nm, and emission at 535 nm. The results are expressed in permeability or Pe in 10^{-3} cm/min. The barrier is considered permeable or open when the Pe of LY is above $0.6x10^{-3}$ cm/min. During each 1 hr experiment, the average cleared volume was plotted versus time and the slope estimated by linear regression analysis. The slope of the clearance curve for control filters with collagen type IV-fibronectin coating was denoted PSf and the slope of the clearance curve for filters with brain endothelial cell monolayers was denoted PSt. The PS value for the endothelial monolayer (PSe) was calculated from: Please click here to view a larger version of this figure.

$$\frac{1}{Pse} = \frac{1}{Pst} - \frac{1}{Psf}$$

The PSe values were divided by the area of the porous membrane (1.1 cm^2 for Millipore filters of 12-well plates) and the result was the permeability coefficient (Pe) with an average of 0.26 ± 0.11 x 10^{-3} cm/min. Results are presented with a vertical scatter plot representation for n = 90 assays (mean of n = 3 to n = 6 monolayers per assay).

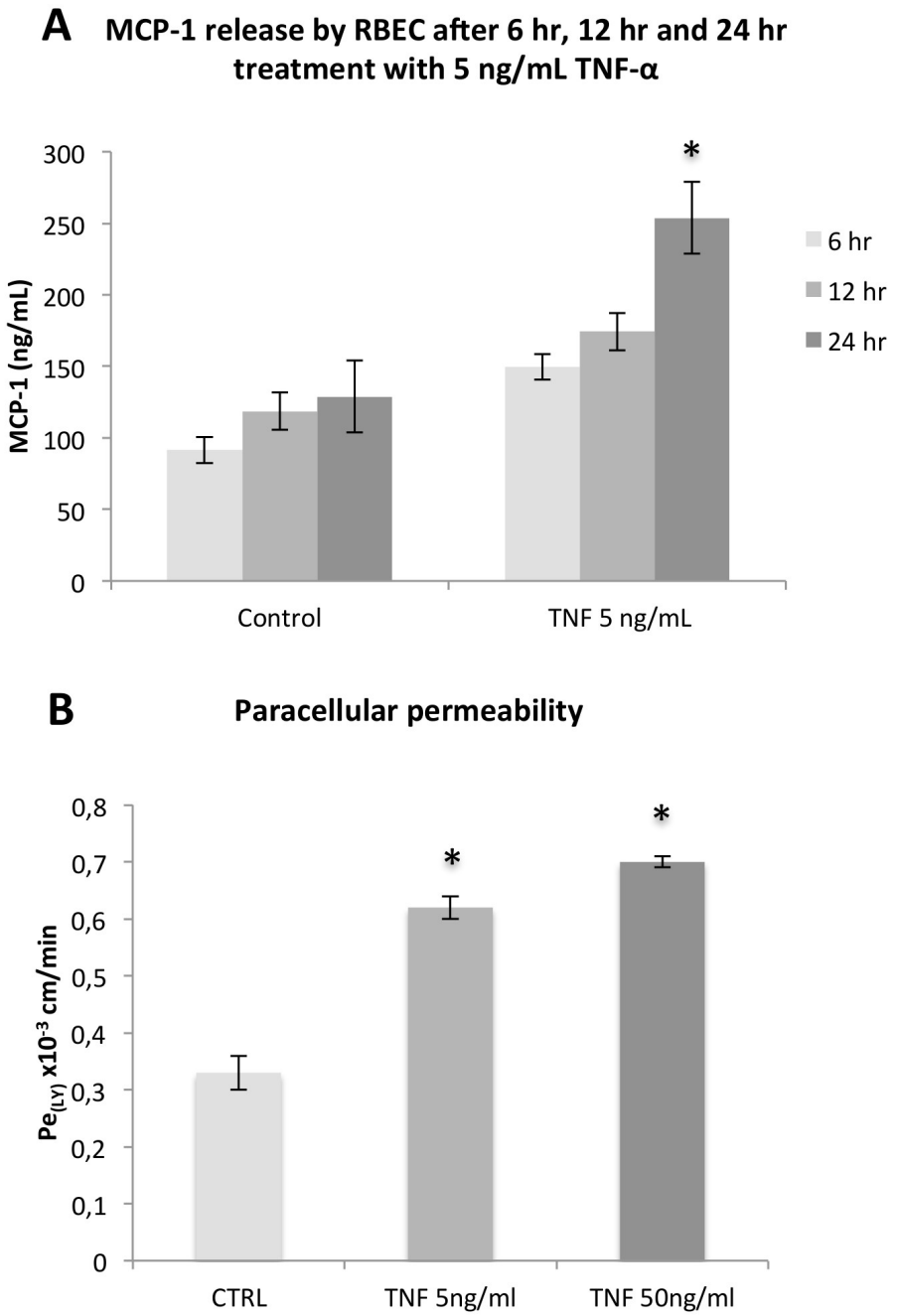

Figure 5. ***In vitro*** **BBB model response to treatment with the pro-inflammatory agent TNF-α.** The culture media from the culture system was replaced just before TNF-α treatment at 5 ng/ml in the upper compartment for 6 hr, 12 hr and 24 hr. CCL2 release by RBEC was quantified in the upper compartment by ELISA assay in comparison with non-treated control. Note that MCP-1 levels increase slightly as a function of time, even in the non-treated wells. Integrity of the endothelial cell barrier measured by endothelial Pe for LY $Pe_{(LY)}$ revealed an increase in monolayer permeability by 24 hr treatment with TNF-α at 5 ng/ml or 50 ng/ml in the range of 0.62 ± 0.02 x 10^{-3} cm/min and 0.7 ± 0.01 x 10^{-3} cm/min respectively, compared to control at 0.33 ± 0.03 x 10^{-3} cm/min (Student's t test, $p < 0.05$).

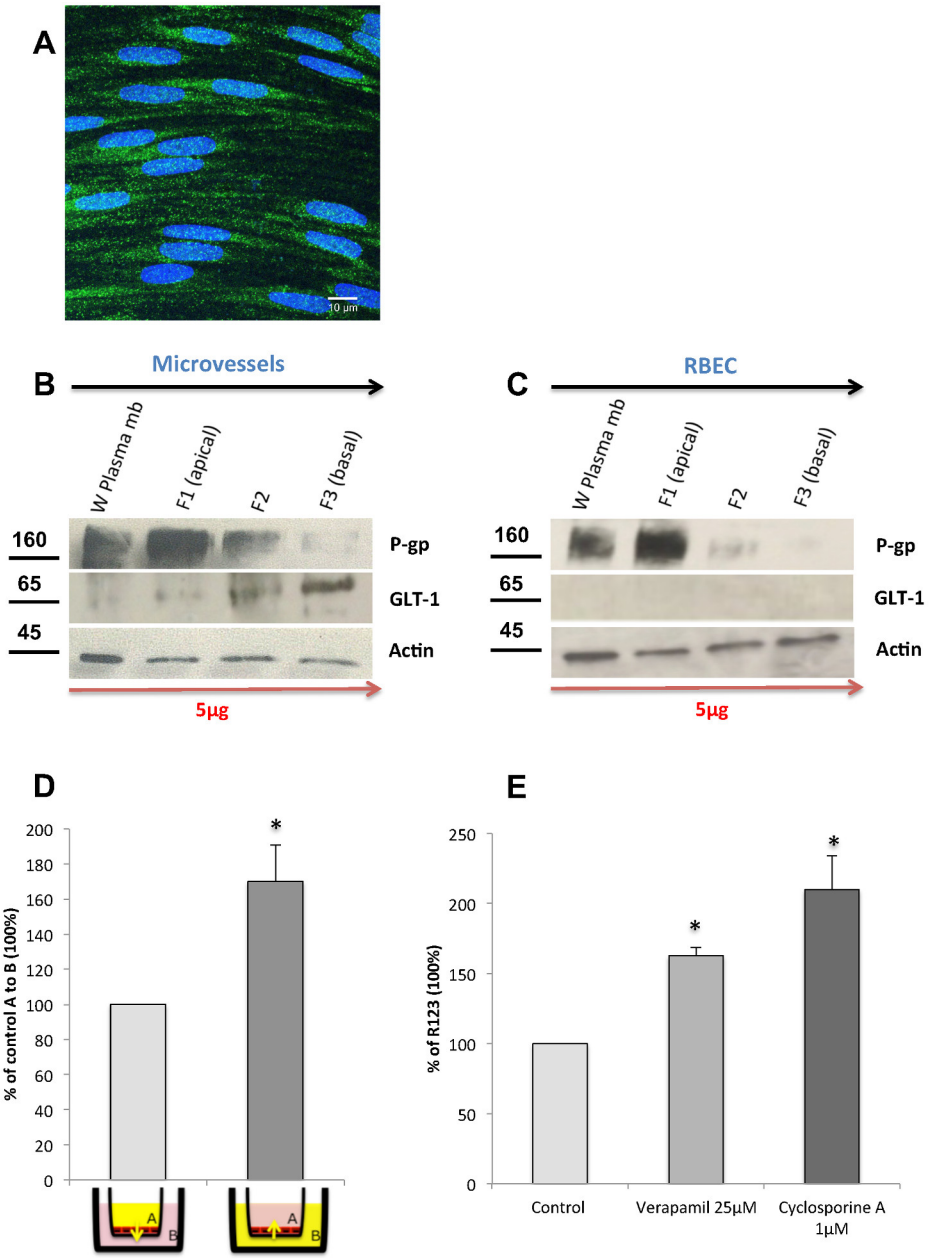

Figure 6. Functionality of the P-gp efflux transporter and RBEC polarization. Expression of the efflux transporter P-gp in brain endothelial cells co-cultured with astrocytes by immunocytochemistry **(A)** and western blot **(B & C)**. Cell membrane proteins were extracted with a cellular protein fractionation kit. Plasma membranes were obtained by hypotonic lysis and differential centrifugations to eliminate organelles and nuclei. Separation of apical and basolateral proteins from plasma membranes were obtained by sucrose density gradient. P-gp was mainly localized in the apical fraction (F1) while Glutamate transporter-1 (GLT-1) was mainly localized in the basolateral fraction (F3). Purified microvessels prior to plating were used as control for the *in vivo* localization of these proteins. Activity of P-gp was determined by measuring the transport polarity of R123, a P-gp ligand. The flux of 1 µM R123 was measured for 1 hr at 37 °C in the luminal-to-abluminal **(A to B)** and in the opposite abluminal-to-luminal **(B to A)** directions. The same experiment was realized without RBEC to assess passive diffusion across the insert filter and data were normalized relative to this value for $Pe_{(R123)}$ calculation (see **Figure 5** legend for Pe calculation method). R123 content in both compartments was measured with a spectrofluorimeter (excitation wavelength at 485 nm, emission wavelength at 535 nm). Data are expressed as 100% of the luminal-to-abluminal transport based on $Pe_{(R123)}$ **(A to B)**. Verapamil (25 µM, 30 min preincubation) and cyclosporine A (1 µM, 30 min preincubation) were used as reference P-gp inhibitors. R123 accumulation in RBEC was measured after 2 hr with or without preincubation with the P-gp inhibitors (Student's t test, $p < 0.05$). Please click here to view a larger version of this figure.

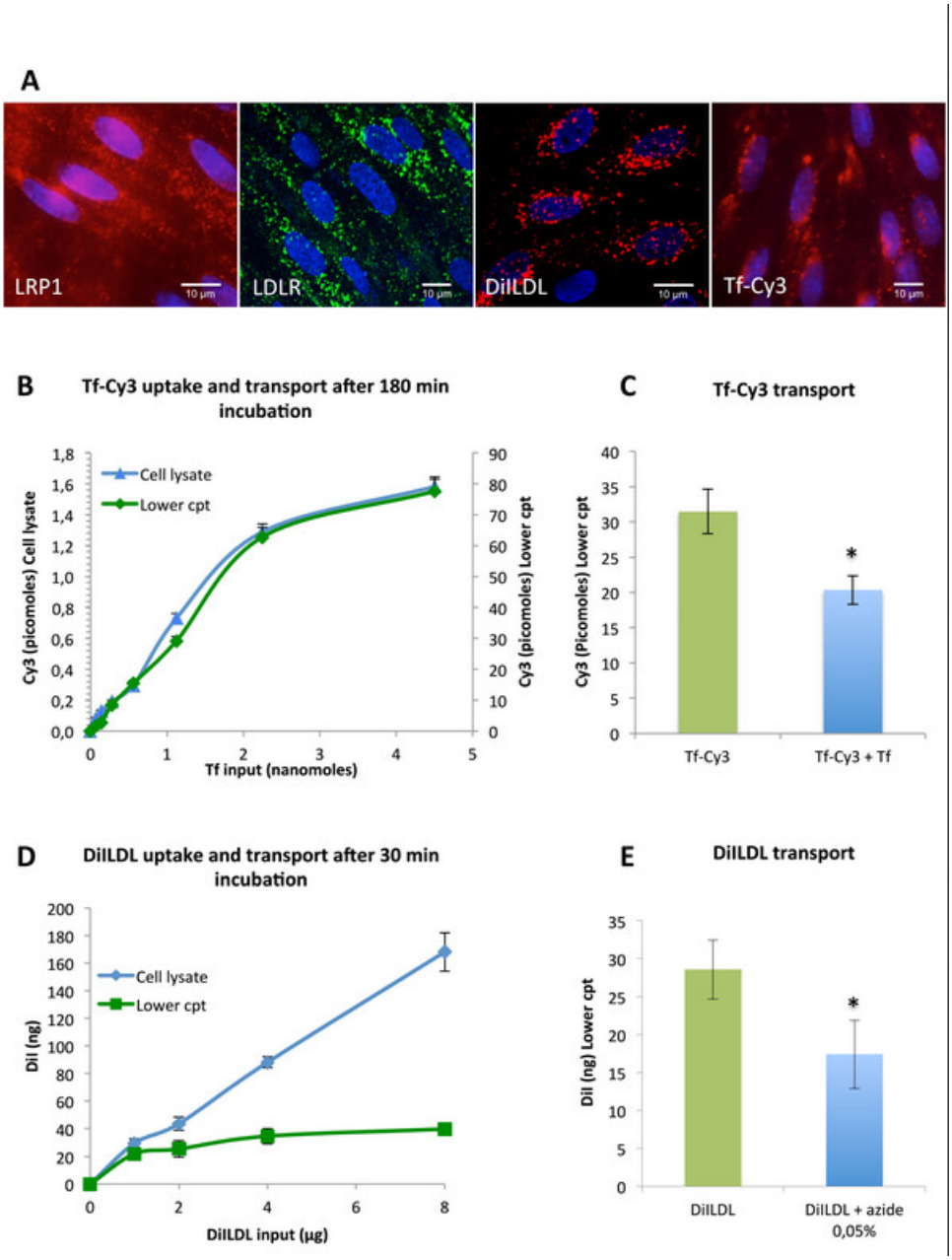

Figure 7. Characterization of receptors involved in Receptor Mediated Transcytosis (RMT). (A) The differentiated RBEC monolayer was immunostained with antibodies against the low density related lipoprotein receptor 1 (LRP1) and the low density lipoprotein receptor (LDLR). Confocal image of RBEC probed for uptake of DiILDL, a fluorescent ligand of the LDLR and for uptake of rat Transferrin-Cy3, a fluorescent ligand of the TfR show punctate staining over the cell surface, with some clustering in the perinuclear region. **(B)** Rat Tf-Cy3 was added to the upper compartment containing the differentiated RBEC monolayer at 75, 150, 300, 600, 1,200, 2,400 and 4,800 picomoles / insert for 180 min at 37 °C (200 µL in the upper compartment and 1,200 µL in the lower compartment). After this time, Cy3 fluorescence was quantified in the cell lysate (200 µL of PBS 0.1 % Triton X100) and in the lower compartment by fluorimetric analysis with a spectrofluorimeter with excitation at 550 nm and emission at 570 nm. Fluorescence units were transformed in picomoles using a linear working range. **(C)** For saturation experiments, rat Tf-Cy3 was added to the upper compartment containing the differentiated RBEC monolayer at 1,200 picomoles / insert for 180 min at 37 °C with or without 15 min pre-incubation with 4,800 picomoles / insert of non-fluorescent Tf. The transport in the lower compartment was quantified as in **(B)** (Student's t test, $p < 0.05$). **(D)** DiILDL was added to the upper compartment containing the differentiated RBEC monolayer at 1, 2, 4 and 8 µg / insert filters for 30 min at 37 °C (200 µl in the upper compartment and 1,200 µl in the lower compartment). After this time, Dil fluorescence was quantified in the cell lysate (200 µl of PBS 0.1 % Triton X100) and in the lower compartment by fluorimetric analysis with a spectrofluorimeter with excitation at 554 nm and emission at 571 nm. Fluorescence units were transformed in µg using a linear working range. **(E)** For transport blocking experiments, sodium azide was added at 0.05% 15 min before the incubation of DiILDL at 2 µg / insert for 30 min at 37 °C. The transport in the lower compartment was quantified as in **(D)** (Student's t test, $p < 0.05$). The absence of toxicity of sodium azide incubation at 0.05% was assessed by $Pe_{(LY)}$ measurement (data not shown). Please click here to view a larger version of this figure.

	Rat brain 5 week old male Wistar rats	Rat spinal cord 5 week old male Wistar rats	Mice brain 5 week old male C57Bl6/RJ
Dispase treatment before meninge removal	no	no	yes (15 min)
Number of animal per experimenter	3	6	5
Liberase DH	1 cortex / 1 mL / tube (60 µg/mL)	2 spinal cord / 1 mL / tube (60 µg/mL)	2,5 cortex / 1 mL / tube (45 µg/mL)
Seeding density	1,5 cortex / T75	3 spinal cords / T75	5 cortex / T25
90 % confluence	3.10^6 cells / T75	3.10^6 cells / T75	1.10^6 Cells / T25
N° of inserts (12-well plates) at 160.10^3 cells / filter	18	18	6
$Pe_{(LY)}$ x 10^{-3} cm/min	0,26 ± 0,11	0,6	0,29 ± 0,10
ZO-1	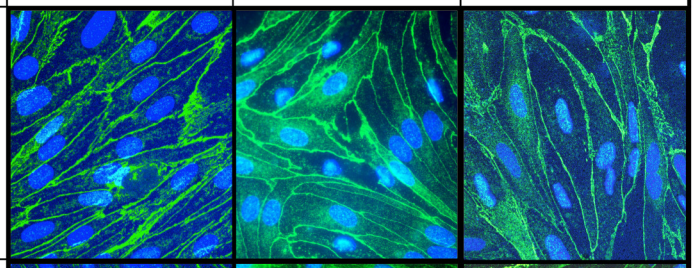		
Occludin	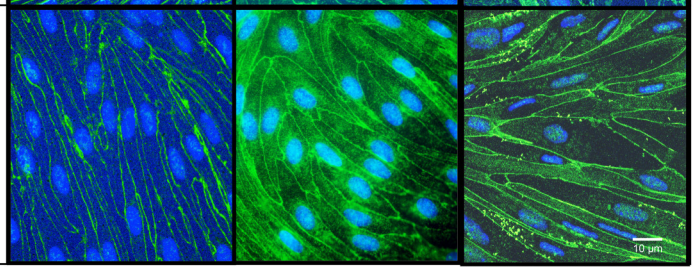		

Figure 8. *In vitro* BBB models from rat spinal cord endothelial cells or from mouse brain. The table highlights important parameters for microvessel extraction from rat brain, rat spinal cord and mouse brain. Photomicrographs show immunostaining for ZO1 and occludin in endothelial cell monolayers prepared from rat brain, rat spinal cord and mouse brain.

Discussion

We describe the implementation of a weekly reproducible protocol for the isolation and plating of brain microvessels, following purification and culture of RBEC and further setting up of co-cultures with primary rat astrocytes to generate an *in vitro* BBB model with characteristic BBB properties.

Successfully establishing standardized *in vitro* BBB cultures requires optimal conditions in the multiple sequential steps of the process. The model was (a) optimized to obtain the lowest paracellular permeability, which remains the “Holy grail” of *in vitro* BBB models, and (b) validated for efflux and RMT mechanisms.

Production, Purification and Proliferation of RBEC

The greatest challenge when cultivating RBEC is to achieve reproducibility between different cultures. Standardization of the protocol requires high quality tools for dissection, high quality reagents and respect of reagent expiration dates. The experimenter needs to be skilled in micro-dissection under stereomicroscope for rapid removal of meninges and large vessels from the cortex surface. Once the brains are isolated and mechanically dissociated, one of the major challenges is the optimal enzymatic digestion of the freshly isolated brain microvessels. The type and quality of the enzymes used is critical. A mix of collagenases type I and II and dispase at high concentration with low variability between batches was used. Also important are the duration of the enzymatic digestion and the ratio between enzyme concentration/tissue weight/volume of digestion. The best yield of brain microvessel production was obtained with the equivalent of cortices from 1 brain in 1 ml of collagenases / dispase mix at 60 µg/ml during both digestions, respectively 30 min and 1 hr.

Also critical is the elimination of contaminating cells (astrocytes and mainly pericytes). These cells proliferate at higher rate than endothelial cells and do not establish tight junctions with the latter, thus preventing the establishment of a homogeneous cell monolayer with good paracellular restrictiveness. Considering that brain endothelial cells express much higher levels of efflux pumps, especially P-gp, compared to the other

cell types found in microvessels, they tolerate better the otherwise toxic concentrations of P-gp ligand drugs, while non-endothelial cells are eliminated. Puromycin treatment at 4 µg/ml for the first two days was followed by two more days at 2 µg/ml to obtain good endothelial cell purity. This selection can also favor capillary endothelial cells versus those from venules, pre-capillary arterioles or larger microvessels, and lead to tighter monolayers. In addition, the use of poor plasma-derived bovine serum is an imperative to obtain pure cultures of endothelial cells[47,48]. The plasma-derived serum lacks platelet-derived growth factor (PDGF), which is mitogenic for fibroblasts, for smooth muscle cells and therefore for pericytes.

We observed that treatment of plastic and filters with a mix of collagen type IV from mice and human fibronectin yields a significant advantage, with a 2-fold increase of the proliferation yield in comparison with the traditionally recommended collagen type I from rat tail. Important cues for cell proliferation are provided by the extracellular matrix such as integrin and growth factor (bFGF) activation[49]. Buffer concentration and pH of the culture media have been described to impact positively on paracellular tightness[50] and we observed a better reproducibility between cultures with the addition of HEPES buffer at 5 mM.

Differentiation of RBEC: Co-culture Establishment on Insert Filters

Once brain endothelial cells have been purified and have proliferated for 6 days, they can be plated on filters. Cell plating at high density is critical to obtain a perfect monolayer. A seeding density of $160x10^3$ cells per 12 well plate filters was necessary and sufficient to obtain a confluent monolayer 24 hr after seeding. However, isolation of primary brain capillary endothelial cells from their environment is a paradox in the construction of a BBB *in vitro* model as it is known that primary cells, and notably brain capillary endothelial cells, are strongly regulated by their environment and inductive factors produced by the different surrounding cell types. Brain capillary endothelial cells cultured alone rapidly de-differentiate and loose some specific brain endothelial markers. Thus, primary endothelial cells should be used at low passage (P1) and re-connected, at least in part, with their environment by co-culture with astrocytes or medium conditioned by astrocytes[47,51]. This holds true for astrocyte differentiation as brain endothelial cells and astrocytes are involved in two-way induction. Culturing RBEC with astrocytes led to strong induction of interendothelial TJ[52,23]. The molecular mechanisms of re-induction remain largely unknown, and research is ongoing in several laboratories to identify specific modulating factors secreted by astrocytes, which could promote optimal endothelial cell differentiation[53,54]. Factors secreted by brain endothelial cells including leukemia inhibitory factor (LIF) have been shown to induce astrocytic differentiation[55,56]. Before co-culture establishment, astrocytes were exposed to differentiation medium containing the glucocorticoid receptor agonist hydrocortisone, and co-culture conditioned medium. Hydrocortisone is known to improve the tightness of brain endothelial cells and is used in BBB models especially from rat[57] and mouse[58,59] endothelial cells. The conditioned medium is collected from the lower compartment of the endothelial cell/astrocyte co-culture system after 3 days and frozen for later use. The use of co-culture conditioned medium reduced the time of endothelial cell differentiation to 3 days with optimal paracellular permeability for 2 more days and also improved reproducibility between cultures.

Overall, the protocol we describe yields a reproducible TEER over 300 ohm · cm^2 and an average paracellular permeability coefficient $Pe_{(LY)}$ of $0.26 \pm 0.11 \times 10^{-3}$ cm/min, similar to the best primary cell-based BBB models[22,12]. The protocol we describe in the present manuscript with the proposed modulation of microvessel enzymatic digestion can be extended to endothelial cells from the rat spinal cord[60] and from mice brain.

Molecular and Functional Characterization

In addition to TJ induction, astrocytes also contribute to the expression of efflux transporters such as P-gp in brain endothelial cells[61]. We indeed show expression of the efflux transporter P-gp in the BBB model and we demonstrate the polarity of the P-gp efflux pump localization using biochemical approaches, and of P-gp activity using a functional assay. GLT-1 expression was detected in the basal membrane fraction of microvessels but was not detected in cultured RBEC. We hypothesize that GLT-1 was down regulated in our RBEC culture in comparison with *in vivo* conditions and consequently not detectable by western blot analysis. Excess glutamate is neurotoxic and *in vivo,* GLT-1 is responsible for glutamate efflux from the basal compartment (parenchyma) to the apical compartment (blood circulation). In astrocyte cultures, GLT-1 expression remains very low and is induced by the addition of glutamate in the medium[62,63].

We also confirm the expression of influx transporters at the apical membrane such as LRP1, LDLR and TfR. Functionality of TfR and LDLR was demonstrated with binding and transport experiments of Tf-Cy3 and DiLDL from the luminal to the abluminal side of the monolayer as previously shown with a bovine *in vitro* BBB model[64]. Interestingly, it has been shown that lipid requirement from astrocytes increases the expression of LDLR on brain capillary endothelial cells[65,66] further confirming the physiological crosstalk between astrocytes and brain endothelial cells, including *in vitro.* We have chosen to exemplify transport with fluorescent dyes such as Cy3 and DiI considering that spectrofluorimetric analysis is available in most laboratories, and can prove useful to validate *in vitro BBB* models. However, quantification of fluorescence is far less sensitive than radioactivity and requires an increase in the number of experiments to obtain significant data. Ideally, Tf and LDL are usually radiolabeled (Iodine 125) for such binding/uptake and transport experiments.

We also show that the differentiated endothelial cell monolayer obtained with the proposed protocol responds to inflammation induced by TNF-α, as revealed by CCL2 release and BBB opening. CCL2 (MCP-1) and its receptor CCR2 are involved in CNS pathologies such as multiple sclerosis, experimental autoimmune encephalomyelitis (EAE)[67], CNS trauma[68] and are known as mediators of leukocyte migration into the CNS under neuroinflammatory conditions[69,70]. With the tested protocol, we cannot conclude on a polarized secretion of CCL2 because BBB opening allows the CCL2 concentration to equilibrate between both upper (apical) and lower (basal) compartments. Consequently, we clearly underestimate the amount of CCL2 produced by the RBEC in the apical compartment at 24 hr (**Figure 5A**).

General Overview and Limitations of BBB *In Vitro* Models: *In Vivo* versus *In Vitro* and Rodent versus Human Comparisons

Many promising CNS drugs that proved effective in BBB passage *in vitro* failed in clinical trials due to lack of predictability from *in vitro* BBB models often based on cells isolated from other species than human. To the best of our knowledge, the *in vitro* BBB models are probably more predictive when it comes to studying mechanistic aspects of protein networks, signal transduction, transporters and receptors. Every mechanism, pathway or target to be studied *in vitro* has to be characterized for its regulation by complementary environmental cues (other cell

types, chemicals, proteins) and combined to *in situ* studies with the same animal species, and when possible, with microvessels and endothelial cells isolated from humans, with the restrictions and caution evoked below.

In vitro BBB models have to be seen as autonomous systems, isolated from body regulation, but still endowed with major *in vivo* properties and a potential for regulation by environmental cues. No "ideal" *in vitro* BBB model has been proposed yet[71,72,73] because the endothelial cell monolayers lack a number of important constituents of the neuro-glia vascular unit (NGVU) and are isolated from blood and body regulation. The lack of pericytes[74,16] or neurons[17,18] or the different constituents of the extracellular matrix used for plastic coating or the culture medium and serum used for cell growth in the most common and "easiest made" *in vitro* BBB models based on endothelial cells differentiated with astrocytes may modulate protein expression in comparison with the *in* vivo situation[75]. These models may express many transporters displayed *in vivo*, but not all. In some cases, transport parameters were first verified in isolated microvessels (closest to the *in vivo* situation), and then studied in cell culture systems[76,61].

Molecular biology research has allowed the characterization of gene and protein expression in isolated microvessels and low passage endothelial cell cultures from the same species, and between different species, most often from small animals such as rodents (mice and rats) or from cow and pig in comparison to humans[77,78,75,15]. Transcriptomic comparison between *in vivo* and *in vitro* brain microvascular endothelial cells showed numerous gene transcripts that were differentially expressed and most often significantly downregulated *in vitro*. Transcripts encoding influx transporters such as TfR and proteins implicated in vesicle trafficking are mainly downregulated in cultured brain endothelial cells, suggesting a general decrease in endocytosis and vesicular transport in such cells. Culture manipulation in terms of purity (puromycin treatment) and treatment with hydrocortisone may help to restore a more "*in vivo*-like" gene expression profile[77]. Transcriptomic studies also revealed important differences between species that further complicate predictions on drug uptake in humans based on rodent *in vitro* BBB models[75]. *In vitro* BBB models involving co-culture of human endothelial cells and astrocytes have been described[15]. Although relevant, these models are more difficult to implement on a regular basis as they require regulated access to post-mortem human tissue and there is heterogeneity in the quality/properties of the human brain endothelial cells depending on the age, diseases, and possibly medical treatment of donors. Efforts have to be made to develop new *in vitro* models that better reproduce the physiological, anatomical and functional characteristics of the *in vivo* BBB. Co-cultures involving three-cell types are highly restrictive and appear difficult to implement routinely. To date, the most complex *in vitro* BBB models are the dynamic *in vitro* models (DIV-BBB) which include vessel-like organization with astrocytes and include a flow of medium that mimics the blood flow [75,79,80,81,82,83,84,85]. When cerebral endothelial cells are exposed to a flow, the generated shear stress activates mechanotransducers at the cell surface, which modulate the expression of different genes involved in endothelial cell physiology such as cell division, differentiation, migration and apoptosis[80]. *In vivo,* shear stress generated by the blood flow is responsible for mitotic arrest at the cell contact, which permits the establishment of an endothelial cell monolayer in blood vessels[80]. Genomic and proteomic analysis of normal human brain microvascular endothelial cells showed the impact of shear stress in BBB endothelial physiology[84]. Shear stress is responsible for cell survival, a higher degree of endothelial cell adhesion, efflux pump induction and better polarization of transporters[75], regulation of glucose metabolism[75,86], oxidation mediated by CYP450 enzymes[75] and the regulation of paracellular permeability by increasing the expression of genes encoding for intercellular junctional elements like occludin and ZO-1[87,75,80] and consequently high TEER around 1,500 - 2,000 ohm · cm^2, the closest to known *in vivo* parameters[79,80]

In the biotechnology and pharmaceutical industry, routine screening of drugs or even high throughput screening (HTS) and efforts to reduce animal experimentation, led to the development of different cell lines to be used in replacement of the primary culture of cerebral endothelial cells which remain more difficult to set-up routinely. In most cases, primary cultures of cerebral endothelial cells were transduced with an immortalizing gene (SV40 or polyoma virus large T-antigen or adenovirus E1A), either by transfection of plasmid DNA or by infection using retroviral vectors[88,89,75]. Several endothelial cell lines of cerebral origin have been developed such as the RBE4, GP8/3.9, GPNT, RBEC1, TR-BBBs or rBCEC4 rat cell lines[88,75], the b.End3 mouse cell line[90,75], the *PBMEC/C1–2* porcine cell line[87,75], and the hCMEC/D3 human cell line[89,75]. Other models are based on cells of non-cerebral origin such as the Madin-Darby canine kidney (MDCK) or Caco2 cell lines[12,75]. Among the different human cerebral endothelial cell lines, the hCMEC/D3 has been widely cited and improved as a model of BBB since its establishment in 2005[91,92]. Like primary cultures, cell lines present advantages and limitations. They are easier to handle than primary cultures, have an extended life span, are well characterized and allow reproducibility between large scale experiments. However, cell lines can lose tissue-specific functions, lose environmental regulation and acquire a molecular phenotype quite different from cells *in vivo*[75,89]. In particular, monolayers generated from cell lines present reduced tightness, low TEER and show transporter profile variation[75,89]. Thus animal experiments or studies in primary cells are often preferred despite their added complexity.

Disclosures

Michel Khrestchatisky is director of the UMR7259 laboratory, co-founder and scientific counsel of VECT-HORUS biotechnology company.

Acknowledgments

Financial support to VECT-HORUS is acknowledged from the Fonds Unique Interministériel (FUI/ MEDUL project) and to VECT-HORUS and the UMR7259 laboratory from the Agence Nationale de la Recherche (ANR, TIMPAD, VECtoBrain, VEC2Brain, ADHOC and PREVENTAD collaborative projects). The UMR7259 laboratory also acknowledges financial support from the CNRS and from Aix-Marseille Université.

References

1. Rubin, L.L., Staddon, J.M. The cell biology of the blood-brain barrier. *Annu Rev Neurosci.* **22**, 11-28 (1999).
2. Abbott, N.J. Dynamics of CNS barriers: evolution, differentiation, and modulation. *Cell. Mol. Neurobiol.* **25**, 5-23 (2005).
3. Cecchelli, R., *et al.* Modelling of the blood-brain barrier in drug discovery and development. *Nat Rev Drug Discov.* **6** (8), 650-61 (2007).
4. Pekny, M., Stanness, K.A., Eliasson, C., Betsholtz, C., Janigro, D. Impaired induction of blood-brain barrier properties in aortic endothelial cells by astrocytes from GFAP-deficient mice. *Glia.* **22** (4), 390-400 (1998).

5. Girouard, H., Iadecola, C. Neurovascular coupling in the normal brain and in hypertension, stroke, and Alzheimer disease. *J Appl Physiol.* **100** (1), 328-35 (2006).
6. Dehouck, M.P., Méresse, S., Delorme, P., Fruchart, J.C., Cecchelli, R. An easier, reproducible, and mass-production method to study the blood-brain barrier *in vitro*. *J Neurochem.* **54** (5), 1798-801 (1990).
7. Culot, M., *et al.* An *in vitro* blood-brain barrier model for high throughput (HTS) toxicological screening. *Toxicol In Vitro.* **22** (3), 799-811 (2008).
8. Zhang, Y., *et al.* Porcine brain microvessel endothelial cells as an *in vitro* model to predict *in vivo* blood-brain barrier permeability. *Drug Metab Dispos.* **34** (11), 1935-43 (2006).
9. Patabendige, A., Skinner, R.A., Abbott, N.J. Establishment of a simplified *in vitro* porcine blood-brain barrier model with high transendothelial electrical resistance. *Brain Res.* **1521**, 1-15 (2012).
10. Abbott, N.J., Dolman, D.E., Drndarski, S., Fredriksson, S.M. An improved *in vitro* blood-brain barrier model: rat brain endothelial cells co-cultured with astrocytes. *Methods Mol Biol.* **814**, 415-30 (2012).
11. Nakagawa, S., *et al.* A new blood-brain barrier model using primary rat brain endothelial cells, pericytes and astrocytes. *Neurochem Int.* **54** (3-4), 253-63 (2009).
12. Wilhelm, I., Fazakas, C., Krizbai, I.A. *In vitro* models of the blood-brain barrier. *Acta Neurobiol Exp (Wars).* **71** (1), 113-28 (2011).
13. Coisne, C., *et al.* Mouse syngenic *in vitro* blood-brain barrier model: a new tool to examine inflammatory events in cerebral endothelium. *Lab Invest.* **85** (6), 734-46 (2005).
14. Josserand, V., *et al.* Evaluation of drug penetration into the brain: a double study by *in vivo* imaging with positron emission tomography and using an *in vitro* model of the human blood-brain barrier. *J Pharmacol Exp Ther.* **316** (1), 79-86 (2006).
15. Lacombe, O., *et al. In vitro* primary human and animal cell-based blood-brain barrier models as a screening tool in drug discovery. *Mol Pharm.* **8** (3), 651-63 (2011).
16. Nakagawa, S., *et al.* Pericytes from brain microvessels strengthen the barrier integrity in primary cultures of rat brain endothelial cells. *Cell Mol Neurobiol.* **27** (6), 687-94 (2007).
17. Lippmann, E.S., Weidenfeller, C., Svendsen, C.N., Shusta, E.V. Blood-brain barrier modeling with co-cultured neural progenitor cell-derived astrocytes and neurons. *J Neurochem.* **119** (3), 507-20 (2011).
18. Xue, Q., *et al.* A novel brain neurovascular unit model with neurons, astrocytes and microvascular endothelial cells of rat. *Int J Biol Sci.* **9** (2), 174-89 (2013).
19. Sohet, F., Daneman, R. Genetic mouse models to study blood-brain barrier development and function. *Fluids Barriers CNS.* **10** (1), 3 (2013).
20. Shayan, G., Choi, Y.S., Shusta, E.V., Shuler, M.L., Lee, K.H. Murine *in vitro* model of the blood-brain barrier for evaluating drug transport. *Eur J Pharm Sci.* **42** (1-2), 148-55 (2011).
21. Cecchelli, R., *et al. In vitro* model for evaluating drug transport across the blood-brain barrier. *Adv Drug Deliv Rev.* **36** (2-3), 165-178 (1999).
22. Deli, M.A., Abrahám, C.S., Kataoka, Y., Niwa, M. Permeability studies on *in vitro* blood-brain barrier models: physiology, pathology, and pharmacology. *Cell Mol Neurobiol.* **25** (1), 59-127 (2005).
23. Perrière, N., *et al.* A functional *in vitro* model of rat blood-brain barrier for molecular analysis of efflux transporters. *Brain Res.* **1150**, 1-1 (2007).
24. Pardridge, W.M., Buciak, J.L., Friden, P.M. Selective transport of an anti-transferrin receptor antibody through the blood-brain barrier *in vivo*. *J Pharmacol Exp Ther.* **259** (1), 66-70 (1991).
25. Delbart, C., Fruchart, J.C., Cecchelli, R. Low-density lipoprotein receptor on endothelium of brain capillaries. *J Neurochem.* **53** (2), 340-5 (1989).
26. Gosselet, F., Candela, P., Sevin, E., Berezowski, V., Cecchelli, R., Fenart, L. Transcriptional profiles of receptors and transporters involved in brain cholesterol homeostasis at the blood-brain barrier: use of an *in vitro* model. *Brain Res.* **1249**, 34-42 (2009).
27. Pardridge, W.M. Vector-mediated drug delivery to the brain. *Adv Drug Deliv Rev.* **36** (2-3), 299-321 (1999).
28. Pardridge W.M., Boado, R.J. Reengineering biopharmaceuticals for targeted delivery across the blood-brain barrier. *Methods Enzymol.* **503**, 269-92 (2012).
29. Boado, R.J., Lu, J.Z., Hui, E.K., Sumbria, R.K., Pardridge, W.M. Pharmacokinetics and brain uptake in the rhesus monkey of a fusion protein of arylsulfatase a and a monoclonal antibody against the human insulin receptor. *Biotechnol Bioeng.* **110** (5), 1456-65 (2013).
30. Ito, S., Ohtsuki, S., Terasaki, T. Functional characterization of the brain-to-blood efflux clearance of human amyloid-beta peptide (1-40) across the rat blood-brain barrier. *Neurosci Res.* **56** (3), 246-252 (2006).
31. Demeule, M., *et al.* Identification and design of peptides as a new drug delivery system for the brain. *J Pharmacol Exp Ther.* **324** (3), 1064-72 (2008).
32. Yamada, K., *et al.* The low density lipoprotein receptor-related protein 1 mediates uptake of amyloid beta peptides in an *in vitro* model of the blood-brain barrier cells. *J Biol Chem.* **283** (50), 34554-62 (2008).
33. Gabathuler, R. New *protein vecto*rs for physiological transfer of therape*utic* agents to the central nervous system. *Biol Aujourdhui.* **206** (3), 191-203 (2012).
34. Malcor, J.D., *et al.* Chemical optimization of new ligands of the low-density lipoprotein receptor as potential vectors for central nervous system targeting. *J Med Chem.* **55** (5), 2227-41 (2012).
35. Wang, D., *et al.* Engineering a lysosomal enzyme with a derivative of receptor-binding domain of apoE enables delivery across the blood-brain barrier. *Proc Natl Acad Sci U S A.* **110** (8), 2999-3004 (2013).
36. Spencer, B.J., Verma, I.M. Targeted delivery of proteins across the blood-brain barrier. *Proc Natl Acad Sci U S A.* **104** (18), 7594-9 (2007).
37. Kreuter, J., *et al.* Apolipoprotein-mediated transport of nanoparticle-bound drugs across the blood-brain barrier. *J Drug Target.* **10** (4), 317-25 (2002).
38. Stamatovic, S.M., Keep, R.F., Andjelkovic, A.V. Brain endothelial cell-cell junctions: how to 'open' the blood brain barrier. *Curr Neuropharmacol.* **6** (3), 179-92 (2008).
39. Petty, M.A., Lo, E.H. Junctional complexes of the blood-brain barrier: permeability changes in neuroinflammation. *Prog Neurobiol.* **68** (5), 311-23 (2002).
40. Stephan, D., *et al.* TWEAK/Fn14 pathway modulates properties of a human microvascular endothelial cell model of blood brain barrier. *J Neuroinflammation.* **10** (9) (2013).
41. Descamps, L., Cecchelli, R., Torpier, G. Effects of tumor necrosis factor on receptor-mediated endocytosis and barrier functions of bovine brain capillary endothelial cell monolayers. *J Neuroimmunol.* **74** (1-2), 173-84 (1997).

42. Miller, F., *et al.* The MAP kinase pathway mediates transcytosis induced by TNF-alpha in an *in vitro* blood-brain barrier model. *Eur J Neurosci.* **22** (4), 835-44 (2005).
43. Fillebeen, C., Dehouck, B., Benaïssa, M., Dhennin-Duthille, I., Cecchelli, R., Pierce, A. Tumor necrosis factor-alpha increases lactoferrin transcytosis through the blood-brain barrier. *J Neurochem.* **73** (6), 2491-500 (1999).
44. Zhang, Y., Schuetz, J.D., Elmquist, W.F., Miller, D.W. Plasma membrane localization of multidrug resistance-associated protein homologs in brain capillary endothelial cells. J *Pharmacol Exp Ther.* **311** (2), 449-55 (2004).
45. Kane, R.L., Martínez-López, I., DeJoseph, M.R., Viña, J.R., Hawkins, R.A. Na(+)-dependent glutamate transporters (EAAT1, EAAT2, and EAAT3) of the blood-brain barrier. A mechanism for glutamate removal. *J Biol Chem.* **274** (45), 31891-5 (1999).
46. Kannan, R., Mittur, A., Bao, Y., Tsuruo, T., Kaplowitz, N. GSH transport in immortalized mouse brain endothelial cells: evidence for apical localization of a sodium-dependent GSH transporter. *J Neurochem.* **73** (1), 390-9 (1999).
47. Abbott, N.J., Hughes, C.C., Revest, P.A., Greenwood J. Development and characterisation of a rat brain capillary endothelial culture: towards an *in vitro* blood-brain barrier. *J Cell Sci.* **103** (1), 23-37 (1992).
48. Perrière, N., *et al.* Puromycin-based purification of rat brain capillary endothelial cell cultures. Effect on the expression of blood-brain barrier-specific properties. *J. Neurochem.* **93** (2), 279-89 (2005).
49. Tsou, R., Isik, F.F. Integrin activation is required for VEGF and FGF receptor protein presence on human microvascular endothelial cells. *Mol Cell Biochem.* **224** (1-2), 81-9 (2001).
50. Helms, H.C., Waagepetersen, H.S., Nielsen, C.U., Brodin, B. Paracellular tightness and claudin-5 expression is increased in the BCEC/astrocyte blood-brain barrier model by increasing media buffer capacity during growth. *AAPS J.* **12** (4), 759-70 (2010).
51. Rubin, L.L., Sanes, J.R. Neuronal and glial cell biology. *Curr Opin Neurobiol.* **6** (5), 573-5 (1996).
52. Abbott, N.J. Astrocyte-endothelial interactions at the blood-brain barrier. *Nat Rev Neurosci.* **7** (1), 41-53 (2006).
53. Deracinois, B., *et al.* Glial-cell-mediated re-induction of the blood-brain barrier phenotype in brain capillary endothelial cells: a differential gel electrophoresis study. *Proteomics.* **13** (7), 1185-99 (2013).
54. Haseloff, R.F., Blasig, I.E., Bauer, H.C., & Bauer, H. In search of the astrocytic factor(s) modulating blood-brain barrier functions in brain capillary endothelial cells *in vitro*. *Cell Mol Neurobiol.* **25** (1), 25-39 (2005).
55. Mi, H., Haeberle, H., & Barres, B.A. Induction of astrocyte differentiation by endothelial cells. *J Neurosci.* **21** (5), 1538-47 (2001).
56. Abbott, N.J. Astrocyte endothelial interactions and blood-brain barrier permeability. *J. Anat.* **200** (6), 629 – 638 (2002).
57. Calabria, A.R., Weidenfeller, C., Jones, A.R., de Vries, H.E., Shusta, E.V. Puromycin-purified rat brain microvascular endothelial cell cultures exhibit improved barrier properties in response to glucocorticoid induction. *J Neurochem.* **97** (4), 922-33 (2006).
58. Förster, C., *et al.* Occludin as direct target for glucocorticoid-induced improvement of blood-brain barrier properties in a murine *in vitro* system. *J. Physiol.* **565** (Pt. 2), 475 (2005).
59. Förster, C., Waschke, J., Burek, M., Leers, J., Drenckhahn, D. Glucocorticoid effects on mouse microvascular endothelial barrier permeability are brain specific. *J. Physiol.* **573** (Pt. 2), 413 (2006).
60. Ge, S., Pachter, J.S. Isolation and culture of microvascular endothelial cells from murine spinal cord. *J Neuroimmunol.* **177** (1-2), 209-14 (2006).
61. Berezowski, V., Landry, C., Dehouck, M.P., Cecchelli, R., Fenart, L. Contribution of glial cells and pericytes to the mRNA profiles of P-glycoprotein and multidrug resistance-associated proteins in an *in vitro* model of the blood-brain barrier. *Brain Res.* **1018** (1), 1-9 (2004).
62. Duan, S., Anderson, C.M., Stein, B.A., Swanson, R.A. Glutamate induces rapid upregulation of astrocyte glutamate transport and cell-surface expression of GLAST. *J Neurosci.* **19** (23), 10193-200 (1999).
63. Gegelashvili, G., Dehnes, Y., Danbolt, N.C., Schousboe, A. The high-affinity glutamate transporters GLT1, GLAST, and EAAT4 are regulated via different signalling mechanisms. *Neurochem Int.* **37** (2-3), 163-70 (2000).
64. Candela, P., *et al.* Physiological pathway for low-density lipoproteins across the blood-brain barrier: transcytosis through brain capillary endothelial cells *in vitro*. *Endothelium.* **15** (5-6), 254-64 (2008).
65. Dehouck, B., Dehouck, M.P., Fruchart, J.C., Cecchelli, R. Upregulation of the low density lipoprotein receptor at the blood-brain barrier: intercommunications between brain capillary endothelial cells and astrocytes. *J Cell Biol.* **126** (2), 465-73 (1994).
66. Dehouck, B., Fenart, L., Dehouck, M.P., Pierce, A., Torpier, G., Cecchelli, R. A new function for the LDL receptor: transcytosis of LDL across the blood-brain barrier. *J Cell Biol.* **138** (4), 877-89 (1997).
67. Mahad, D.J., Ransohoff, R.M. The role of MCP-1 (CCL2) and CCR2 in multiple sclerosis and experimental autoimmune encephalomyelitis (EAE). *Semin Immunol.* **15** (1), 23-32 (2003).
68. Glabinski A.R., Ransohoff, R.M. Chemokines and chemokine receptors in CNS pathology. *J Neurovirol.* **5** (1), 3-12 (1999).
69. Stamatovic, S.M., *et al.* Monocyte chemoattractant protein-1 regulation of blood-brain barrier permeability. *J Cereb Blood Flow Metab.* **25** (5), 593-606 (2005).
70. Semple, B.D., Kossmann, T., Morganti-Kossmann, M.C. Role of chemokines in CNS health and pathology: a focus on the CCL2/CCR2 and CXCL8/CXCR2 networks. *J Cereb Blood Flow Metab.* **30** (3), 459-73 (2010).
71. Veszelka, S., Nakagawa, S., Niwa, M., Deli, M.A. Patented *in vitro* blood-brain barrier models in CNS drug discovery. *Recent Pat CNS Drug Discov.* **6** (2), 107-118 (2011).
72. Patabendige, A. The value of *in vitro* models of the blood-brain barrier and their uses. *Altern Lab Anim.* **40** (6), 335-8 (2012).
73. Ogunshola, O.O. *In vitro* modeling of the blood-brain barrier: simplicity versus complexity. *Curr Pharm Des.* **17** (26), 2755-61 (2011).
74. Vandenhaute, E., *et al.* Modelling the neurovascular unit and the blood-brain barrier with the unique function of pericytes. *Curr Neurovasc Res.* **8** (4), 258-69 (2011).
75. Shawahna, R., Decleves, X., Scherrmann, J.M. Hurdles with using *in vitro* models to predict human blood-brain barrier drug permeability: a special focus on transporters and metabolizing enzymes. *Curr Drug Metab.* **14** (1), 120-36 (2013).
76. Vernon, H., Clark, K., Bressler, J.P. *In vitro* models to study the blood brain barrier. *Methods Mol Biol.* **758**, 153-68 (2011).
77. Calabria, A.R., Shusta, E.V. A genomic comparison of *in vivo* and *in vitro* brain microvascular endothelial cells. *J Cereb Blood Flow Metab.* **28** (1), 135-48 (2008).
78. Uchida, Y., Ohtsuki, S., Kamiie, J., Terasaki, T. Blood-brain barrier (BBB) pharmacoproteomics: reconstruction of *in vivo* brain distribution of 11 P-glycoprotein substrates based on the BBB transporter protein concentration, *in vitro* intrinsic transport activity, and unbound fraction in plasma and brain in mice. *J Pharmacol Exp Ther.* **339** (2), 579-88 (2011).
79. Cucullo, L., Aumayr, B., Rapp, E., Janigro, D. Drug delivery and *in vitro* models of the blood-brain barrier. *Curr Opin Drug Discov Devel.* **8** (1), 89-99 (2005).
80. Naik, P., Cucullo, L. *In vitro* blood-brain barrier models: current and perspective technologies. *J Pharm Sci.* **101** (4), 1337-54 (2012).

81. Stanness, K.A., et *al*. A new model of the blood--brain barrier: co-culture of neuronal, endothelial and glial cells under dynamic conditions. *Neuroreport.* **10** (18), 3725-31 (1999).
82. Santaguida, S., *et al*. Side by side comparison between dynamic versus static models of blood-brain barrier *in vitro*: a permeability study. *Brain Res.* **1109** (1), 1-13 (2006).
83. Cucullo, L., Marchi, N., Hossain, M., Janigro, D. A dynamic *in vitro* BBB model for the study of immune cell trafficking into the central nervous system. *J Cereb Blood Flow Metab*. **31** (2), 767-77 (2011).
84. Cucullo, L., Hossain. M., Puvenna, V., Marchi, N., Janigro, D. The role of shear stress in Blood-Brain Barrier endothelial physiology. *BMC Neurosci.* **12** (40), (2011).
85. Cucullo, L., Hossain, M., Tierney, W., Janigro, D. A new dynamic *in vitro* modular capillaries-venules modular system: cerebrovascular physiology in a box. *BMC Neurosci.* 14:18 (2013).
86. Qutub, A.A., Hunt, C.A. Glucose transport to the brain: a systems model. *Brain Res Brain Res Rev.* **49** (3), 595-617 (2005).
87. Neuhaus, W.,et *al*. A novel flow based hollow-fiber blood-brain barrier *in vitro* model with immortalised cell line PBMEC/C1-2. *J Biotechnol.* **125** (1), 127-41 (2006).
88. Roux, F., Couraud, P.O. Rat brain endothelial cell lines for the study of blood-brain barrier permeability and transport functions. *Cell Mol Neurobiol*. **25** (1), 41-58 (2005).
89. Weksler, B.B., *et al*. Blood-brain barrier-specific properties of a human adult brain endothelial cell line. *FASEB J.* **19** (13), 1872-4 (2005).
90. Omidi, Y., et al. Evaluation of the immortalised mouse brain capillary endothelial cell line, b.End3, as an *in vitro* blood-brain barrier model for drug uptake and transport studies. *Brain Res.* **990** (1-2), 95-112 (2003).
91. Weksler, B., Romero, I.A., Couraud, P.O. The hCMEC/D3 cell line as a model of the human blood brain barrier. *Fluids Barriers CNS.* **10** (1), 16 (2013).
92. Cucullo, L., et *al*. Immortalized human brain endothelial cells and flow-based vascular modeling: a marriage of convenience for rational neurovascular studies. *J Cereb Blood Flow Metab.* **28** (2), 312-28 (2008).